

Influence of some additives on Cu layer formation in underpotential and overpotential regions in acidic CuSO_4 solutions

10. Voltammetric investigation and AFM observations of the initial stages of Cu deposition onto polycrystalline Pt electrode in the presence of H_2SeO_3

Dijana Šimkūnaitė*,
Emilija Ivaškevič,
Aleksandras Kaliničenko,
Antanas Steponavičius

*Institute of Chemistry,
A. Goštauto 9,
LT-01108 Vilnius, Lithuania*

Copper electrodeposition from acidic CuSO_4 solution without or with H_2SeO_3 has been studied on a Pt(poly) substrate combining the use of electrochemical (cyclic voltammetry and potential step) and morphological (AFM) techniques. The analysis of the chronoamperometric results has indicated that the Cu electrodeposition process occurs through an instantaneous 3D nucleation and growth limited by diffusion and also that the nucleus number density (N) decreases and the average radius of the nucleus (r_{av}) increases with increasing the bulk concentration of H_2SeO_3 . The AFM images have indicated that in the absence of H_2SeO_3 the surface of substrate, being Cu-precovered because of holding in the Cu UPD region, is covered by randomly distributed Cu clusters of comparable sizes. In the local regions of the surface rather large agglomerates composed of clusters of different diameter have also been observed. In the presence of H_2SeO_3 these agglomerates have been shaped into chain-like structures, while in the surrounding areas a rather homogeneous distribution of elongated clusters and separate particles has been seen. In both cases, the growth of clusters has been found to be favoured in the x - y rather than in the z -direction, especially in a solution containing H_2SeO_3 .

Key words: Cu OPD, first stages of electrodeposition, CuSO_4 solution, H_2SeO_3 , cyclic voltammetry, potential step, AFM

INTRODUCTION

An increasing number of applications are being found for thin and very thin layers of copper in high-technology areas such as plating of printed circuit boards, production of interconnections and conductive tracks on various materials. It is common knowledge that the deposition and the properties of thin and very thin layers depend markedly on the early stages of the metal electrocrystallisation process [1, 2]. The important role of nucleation and growth in the early stages of deposition of Cu is at present well established [1, 2].

The addition agents have also been found to affect the mode of electrocrystallisation of Cu [3–6], like other metals [2]. In this context, selenium(IV) compounds continue to be of considerable utility and are being investigated for a variety of applications, including electrocatalysis [7–10], electrodeposition of thin layers of copper selenides as semiconducting materials [9–14], acceleration of Cu^{2+} discharge at Cu electrode in acidic CuSO_4 solutions [15–17].

While the codeposition of Cu and selenium and the formation of thin layers of copper selenides have been the subject of a large number of investigations [9–14], the influence of selenium on the deposition of Cu and, in particular, on the early stages of Cu

* Corresponding author. E-mail: nemezius@ktl.mii.lt

electrocrystallisation has not been thoroughly studied. Two main differences in the experimental conditions can be revealed for the above cases. First, much less amounts of selenium(IV) compounds, ranging from 10^{-6} to 10^{-4} M at a molar ratio $[\text{Cu(II)}]/[\text{Se(IV)}]$ from 10^3 to 10^5 , have been typically used for the studies of the discharge of Cu^{2+} itself, as compared with the formation of copper selenides when the comparable amounts of Cu(II) and Se(IV) in the working solutions are applied. Secondly, if the study is focused solely on the accelerating action of Se(IV) compound upon Cu^{2+} discharge, a region of lower values of overpotentials has commonly been applied [15–17].

Studies examining the initial stages of Cu deposition in the systems containing selenium onto a foreign substrate have recently emerged, in particular, onto Se-precovered Au(poly) [18] and Pt(poly) [19, 20] electrodes. These reports suggest that the initial stages of Cu electrocrystallisation onto Se-modified Au or Pt electrodes [18–20] are based essentially on the respective charge transfer rates and active sites available on the cathode surface. Traces of selenium on the surface of electrodes appear to influence either of these factors. However, no efforts to study the initial stages of Cu electrocrystallisation onto a foreign substrate in the presence of Se(IV) compounds dissolved in the bulk electrolyte have been found.

Electrochemical techniques are traditionally the methods to study the nucleation and growth process, and they provide the mechanistic and kinetic information [1, 2]. However, the electrochemical techniques are insufficient in providing the structural information. In the circumstances, the application of the electrochemical and structural methods of investigation becomes motivated.

In the present work, which is a continuation of our previous study on Cu underpotential deposition (UPD) onto a polycrystalline Pt(poly) electrode in acidic CuSO_4 solution in the presence of H_2SeO_3 [21], the initial stages of Cu deposition in the range of overpotentials (OPD) were investigated by the electrochemical (cyclic voltammetry and potential step) and structural (*ex situ* AFM) techniques.

EXPERIMENTAL

Deposition system. The working solution was 0.5 M H_2SO_4 + 0.01 M CuSO_4 containing H_2SeO_3 in amounts of $1 \cdot 10^{-3}$ to $5 \cdot 10^{-2}$ mM. The molar ratio $[\text{Cu(II)}]/[\text{Se(IV)}]$ was no less than $2 \cdot 10^2$.

The preparation of the working solution, electrochemical cell and the pretreatment of a working Pt(poly) electrode prior to electrochemical and structural investigations were described elsewhere [21].

The roughness factor (f) of Pt(poly) calculated from the hydrogen adsorption current-potential profile in 0.5 M H_2SO_4 solution was obtained to be 2.05 ± 0.05 .

Electrochemical measurements. Potentiodynamic and potential step measurements were performed using a PI 50-1 potentiostat (Belarus) interfaced through a home-made analogue to a digital converter with a PC (Siemens) and a PR-8 programmer (Belarus). In all cases, the working Pt(poly) electrode first was kept in a solution at a starting potential (E_{start}) for 2 min.

The cyclic voltammograms were started in the far positive E region, at $E_{\text{start}} = +0.85$ V, and driven in the cathodic direction to the value of $+0.25$ V being in the Cu OPD region before reversing to E_{start} , all at a potential scan rate (v) of $2 \cdot 10^{-3}$ V s^{-1} . The potential step experiments were done with $E_{\text{start}} = +0.35$ V being in the Cu UPD region to a desired value of Cu deposition potential (E_{dep}) in the Cu OPD region.

All potentials were reported with respect to the standard hydrogen electrode (SHE). The Nernst potential (E) for the Cu^{2+}/Cu couple was estimated measuring the open-circuit potential (OCP) of a bulk Cu deposit in an unstirred 0.5 M H_2SO_4 + 0.01 M CuSO_4 solution at 20 °C and was found to be $+0.260$ V.

Characterisation of the electrode surface. The reasons for choosing the above values of E_{start} were as follows. Regarding cyclic voltammetry, $E_{\text{start}} = +0.85$ V was taken here, because at this E no evidences for Cu UPD onto a Pt(poly) electrode have been found in the literature [21–24]. Moreover, the electrochemical reactions involving the Pt substrate oxidation and the reduction of formed surface platinum oxide can be ruled out, because oxide formation at Pt in 0.5 M H_2SO_4 solution has recently been shown to start at $E \approx +0.85$ V [25].

The potential step experiments were designed so that Cu nucleation would occur onto a Cu-precovered Pt(poly) surface [24]. The amount of Cu deposited underpotentially (Cu_{UPD}) at $E_{\text{start}} = +0.35$ V was shown to range up to *ca.* one monolayer. It should also be pointed out that although the Cu adlayer was virtually complete, as followed from the standard electrochemical procedures, the structural data have indicated that Cu was not evenly distributed over the entire electrode surface. The inhomogeneities and defects of the Pt(poly) electrode surface appear to initiate the formation of well-defined separate agglomerates. Therefore, it has been concluded that the coexistence of a Cu adlayer and Cu agglomerates or patches is possible [24], in other words, the Cu UPD occurring under the potential-controlled conditions, say, at $+0.35$ V, can be considered in the terms of phase transition following some type of Cu nucleation and growth.

At potentials in the region of +0.35 V, the presence of H_2SeO_3 has resulted in the irreversible adsorption of selenium species onto Pt(poly) being in a zero-valence state ($\text{Se}^{\circ}_{\text{ads}}$) in amounts no more than a few at. % [21, 24]. In general, irreversible adsorption of selenium species onto Pt(poly) from acidic CuSO_4 solutions containing H_2SeO_3 has been reported to occur not only at this E but also at more positive E [21, 24]. The Cu UPD process occurring onto Se-modified Pt(poly) surface has been obtained to lead to the roughening of the surface. The surface morphology has been shown to change only slightly [24].

AFM imaging. Samples for the *ex situ* AFM investigation were prepared as follows. The working Pt(poly) electrode after a pretreatment as described elsewhere [21] was allowed to stand at $E_{\text{start}} = +0.35$ V for 2 min. Then, a single E pulse to $E_{\text{dep}} = +0.23$ V located in the region of Cu overpotentials was applied for 30 s. The AFM observation was performed using a TopoMetric Explorer SPM with a Si_3N_4 tip operating in a contact mode.

RESULTS AND DISCUSSION

Cyclic voltammetry. Figure 1a shows a series of typical quasi-steady voltammetric profiles recorded in the unstirred 0.5 M H_2SO_4 + 0.01 M CuSO_4 solution containing the increasing amounts of H_2SeO_3 . For all the solutions, the electrode potential was scanned negatively from +0.85 V, where no electrochemical reaction involving Cu species is obvious, to E sufficiently negative with respect to E_r to en-

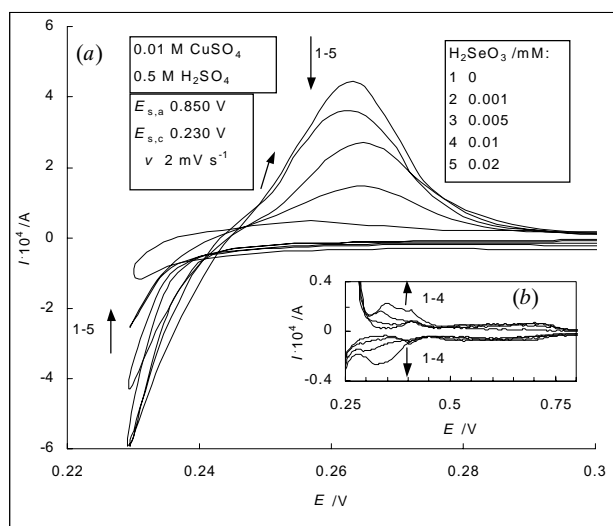


Fig. 1. Typical cyclic voltammograms (1st scan) for Cu bulk deposition and stripping processes (a) and for Cu UPD process (b) onto Pt(poly) electrode in 0.5 M H_2SO_4 + 0.01 M CuSO_4 solution containing increasing amounts of H_2SeO_3 at a scan rate (v) 2 mV s⁻¹

sure Cu deposition, followed by a reversal of a scan to the corresponding bulk stripping of Cu and a return to the E_{start} . The voltammetric responses in the Cu UPD region are also presented for comparison (Fig. 1b). In the overpotential window under study, the cathodic I vs. E curves exhibit one wave. One can see that the cathodic current decreases with increasing the concentration of the additive.

Our observations seem to be consistent with results from other studies of the system Cu + Se [19, 20, 26]. For instance, it is noteworthy that the voltammograms at Pt(poly) exhibit the current loops that are typical of a deposition process requiring nucleation overpotential [27]. Generally, these current loops occur because the metal deposition onto a foreign substrate during cathodic scan requires a considerable overpotential in order to initiate the nucleation and subsequent growth of a deposit. When the scan direction is reversed, the reduction faradaic current continues to flow, because the deposition of metal now takes place on the nucleated surface of a substrate [19, 20, 26–28]. In addition, the effect of H_2SeO_3 upon the current in the Cu UPD region observed here correlates well with the voltammetric data obtained under different conditions [26].

Chronoamperometry. Figures 2 and 3 show a series of current transients for Cu electrodeposition onto Pt(poly) in 0.5 M H_2SO_4 + 0.01 M CuSO_4 solution in the absence or presence of H_2SeO_3 . The shape of these chronoamperograms is typical of a diffusion-limited reaction for the nucleation and growth of a metal deposit onto a foreign substrate [1, 2, 29, 30], exhibiting a rising current due to the growth of a new phase and/or the increasing number of nuclei. The current reaches the maximum (I_{max}) as the diffusion zones of the Cu nuclei begin to overlap, followed by a decaying current which approaches the one corresponding to a planar diffusion to the whole electrode surface.

For 3D nucleation with crystal growth controlled by localized hemispherical diffusion, the following expressions describe the rising and falling portions of the potentiostatic current transients for two extreme cases such as the instantaneous (Eq. 1) and progressive (Eq. 2) nucleation mechanisms, respectively:

$$(I/I_{\text{max}})^2 = 1.9542(t/t_{\text{max}})^{-1}\{1-\exp[-1.2564(t/t_{\text{max}})]\}^2, \quad (1)$$

$$(I/I_{\text{max}})^2 = 1.2254(t/t_{\text{max}})^{-1}\{1-\exp[-2.3367(t/t_{\text{max}})^2]\}^2, \quad (2)$$

where t_{max} is the time at the current maximum [29]. Eqs. (1) and (2) provide a convenient criterion for

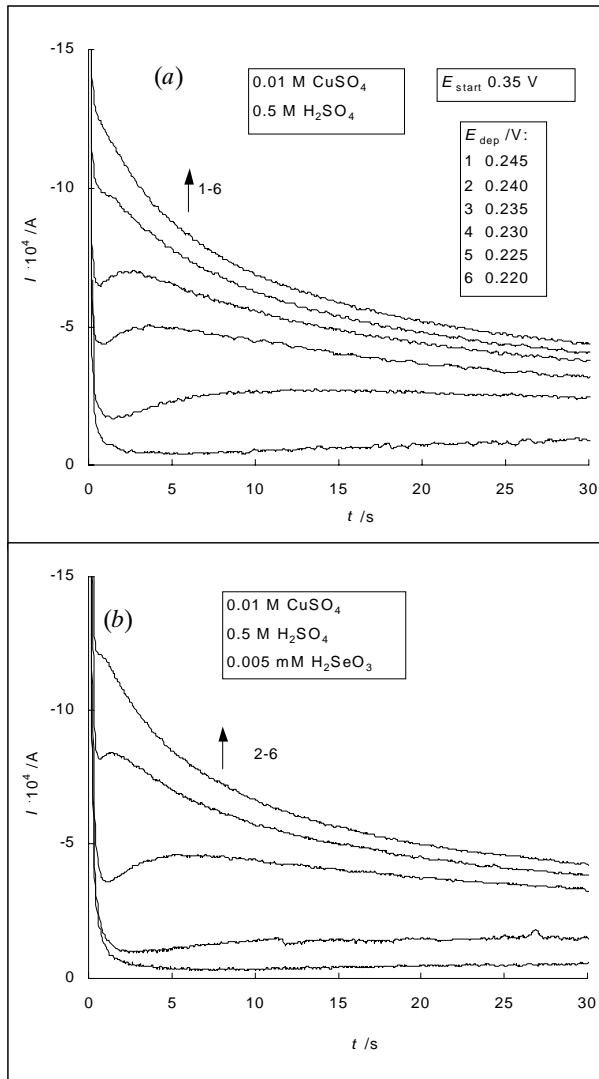


Fig. 2. Potentiostatic current transients for Cu deposition onto Pt(poly) at different values of deposition potential E_{dep} in 0.5 M H_2SO_4 + 0.01 M CuSO_4 solution without (a) or with 0.005 mM H_2SeO_3 (b)

distinguishing between these two extreme cases of nucleation kinetics. The experimental data may be presented in a nondimensional plot, $(I/I_{\text{max}})^2$ vs. t/t_{max} , facilitating comparison with the behaviour predicted for each of the limiting nucleation mechanisms.

Figure 4 shows in these coordinates some of the data obtained in the course of this work. It is evident that the nucleation of Cu onto the Pt(poly) substrate follows closely the response predicted for instantaneous nucleation (Fig. 4a). The same behaviour is observed for a working solution containing H_2SeO_3 (Fig. 4b). The deviation from the predicted responses observed after the maximum, where the process is proposed to be controlled only by linear diffusion, may be associated with a different transition of the hemispherical diffusion to the linear one at different areas of the Pt(poly) electrode surface.

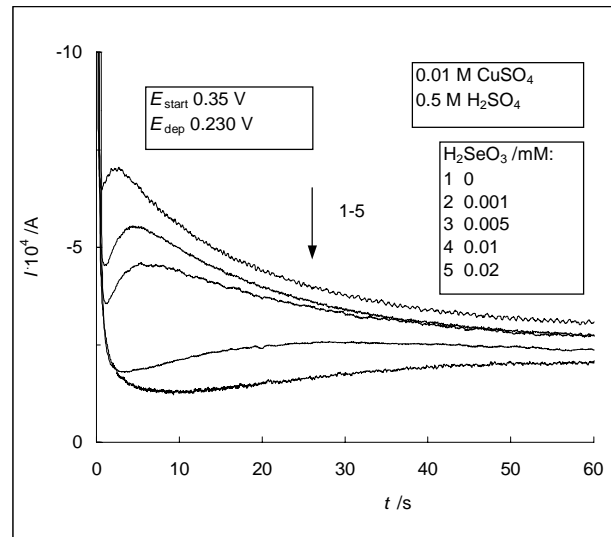


Fig. 3. Potentiostatic current transients for Cu deposition onto Pt(poly) in 0.5 M H_2SO_4 + 0.01 M CuSO_4 solution containing increasing amounts of H_2SeO_3

Once it is established, the instantaneous 3D nucleation with the diffusion-controlled growth model is applicable to Cu electrodeposition; the number of nuclei (N) can be calculated from the values of I_{max} and t_{max} using the following convenient relationship [31]:

$$N = 0.065(zFc / I_{\text{max}} \cdot t_{\text{max}})^2 / k_e, \quad (3)$$

where zF is the molar charge transferred during the electrodeposition, c is the concentration of metal ions, $k_e = (8\pi cM / \rho)^{0.5}$, M and ρ are the molar weight and density of the depositing metal. The parameter k_e for Cu is 0.024.

Assuming that the Cu particles are of spherical shape, the average nuclei radius (r_{av}) can be estimated by applying the following relationship [32]:

$$r_{\text{av}} = (3Qv_m / 4\pi zFN)^{1/3}, \quad (4)$$

where Q is the charge per unit area consumed during the metal electrodeposition and v_m is the molar volume of the depositing metal (for Cu $v_m = 7.1 \text{ cm}^3 \text{ mol}^{-1}$). Q was evaluated by integration of the corresponding chronoamperogram over the time interval up to $t = t_{\text{max}}$ assuming that the contribution of parasitic processes, such as double layer charging, partial reduction of Cu^{2+} and Se(IV), reduction of Se(0) to Se(-II), is negligible under the given experimental conditions.

Considering the instantaneous 3D nucleation process and the Scharifker and Hills model [29], it is possible to recalculate the diffusion coefficient (D) for Cu^{2+} from the product $I_{\text{max}}^2 \cdot t_{\text{max}}$:

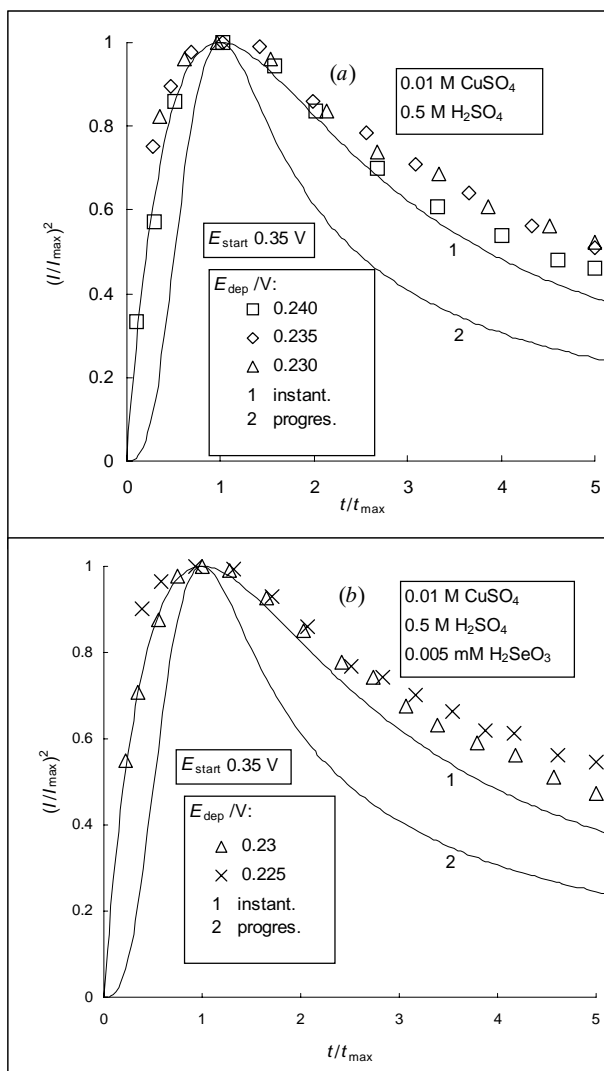


Fig. 4. Comparison of the experimental reduced current-time dependences for Cu nucleation and growth onto Pt(poly) from 0.5 M H₂SO₄ + 0.01 M CuSO₄ solution without (a) or with 0.005 mM H₂SeO₃ (b) to the calculated reduced current-time dependences for the 3D nucleation models developed by Scharifker and Hills

$$I_{\max}^2 \cdot t_{\max} = 0.1629(zFc)^2 D. \quad (5)$$

The calculated values of D for Cu²⁺ ion, N and r_{av} are listed in Table. The calculated D is slightly lower than that reported elsewhere [33]. The origin of this difference is not clear, but a similar discrepancy in diffusion coefficients has also been observed recently for other systems, e.g. for the Zn electro-deposition onto a GC substrate [34]. One can also see that the number of nuclei, 10⁵ to 10⁶ cm⁻², implies rather a low coverage for the Cu nuclei formation, because the calculated value of N corresponds to less than one or *ca.* one in 10⁹ surface atoms from the density of atomic sites (~10¹⁵ cm⁻²) for Pt(poly). Similar results were obtained for the

other values of E_{dep} . So, it can be concluded that only a small fraction of the total number of atomic sites on a Pt(poly) surface is available for the initiation of Cu nucleation and subsequent growth. This is in good agreement with the observations of other authors [23]. N increased with the increase in the Cu overpotential (not shown here), as expected. The data listed in Table also clearly show that N decreases and r_{av} increases with increasing the c of H₂SeO₃.

AFM analysis. The main motive for using AFM in this work was to reveal the morphological characteristics of a Cu deposit after potential stepping and the effect of H₂SeO₃ on the growth mode. As mentioned above, Cu was deposited by a single potential step from $E_{\text{start}} = +0.35$ V to $E_{\text{dep}} = +0.23$ V. The electrolysis was terminated after 10 or 30 s, corresponding to the values of $t/t_{\max} = 3.85$ and 11.5.

The total charges (Q) were calculated to be 6.56 or 15.5 mC in the absence of H₂SeO₃ and 4.77 or 12.3 mC in the presence of 0.005 mM H₂SeO₃, as followed from the chronoamperometric measurements. Such values of Q were suggested to give the amounts of deposited Cu corresponding to about 8 or 20 and 6 or 16 equivalent monolayers, respectively.

Some of the AFM images in 10 × 10 and 2 × 2 μm scales are shown in Fig. 5. Different zones of the surface were imaged for each sample, although only the image for every case is presented here.

It was obtained that, in the H₂SeO₃-free solution, the surface morphology of a Cu deposit after $t_{\text{dep}} = 10$ s was rather similar to that of a Cu-pre-covered Pt(poly) electrode (cf. Ref. 21), *i.e.* the 3D nucleation was not clearly evident during electrodeposition under the above experimental conditions. With the application of the prolonged t_{dep} (30 s), the clusters were found to be of comparable sizes and randomly distributed on the surface with a density of about 9 · 10⁸ cm⁻² (Fig. 5a, c). As one can see, they do not completely merge at these E_{dep} and

Table. Analysis of Cu nucleation process onto Pt(poly) in 0.5 M H₂SO₄ + 0.01 M CuSO₄ solution in the presence of H₂SeO₃ from chronoamperometric data according to the Scharifker and Hills model [29, 30, 32]. $E_{\text{start}} = +0.35$ V, $E_{\text{dep}} = +0.23$ V

H ₂ SeO ₃ , mM	10 ⁴ · I _{max} , A cm ⁻²	t _{max} , s	D for Cu ²⁺ , cm ² s ⁻¹ , from Eq. (5)	10 ⁻⁶ N, cm ⁻² , from Eq. (3)	r _{av} , μm, from Eq. (4)
0	8.23	2.60	2.91 · 10 ⁻⁶	2.20	0.21
0.001	6.52	4.55		1.15	0.29
0.005	5.30	6.10		0.96	0.31
0.01	3.11	27.65		0.14	0.83

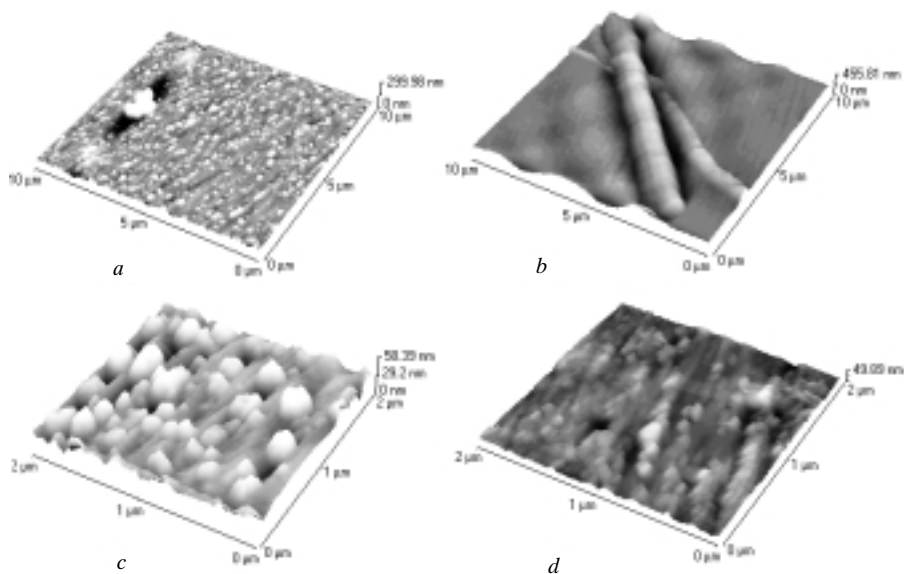


Fig. 5. *Ex situ* AFM images of Pt(poly) surface after Cu deposition at $E_{\text{dep}} = +0.23$ V for 30 s from 0.5 M $\text{H}_2\text{SO}_4 + 0.01$ M CuSO_4 solution without (a, c) or with 0.005 mM H_2SeO_3 (b, d)

t_{dep} . In the local regions of the surface, the rather large agglomerates composed of different diameter clusters are also observed (Figs. 5 and 6). It should be noted that the presence of such agglomerates agrees well with the earlier observations relative to Cu UPD onto Pt(poly) [21], suggesting Cu deposition to be preferentially initiated at most distinct surface defects.

The cross-sectional analysis was further applied to obtain quantitative information about the parameters of surface roughness. Figure 6 shows a cross-sectional profile of the surface along a line as shown in the top-view image. From this profile a lateral distance and height can be determined. The ratio between the growth in the lateral direction and that in the vertical direction (Fig. 6) was found to be more or less the same as in the case of Cu UPD [21]. Standard roughness measurements showed that the arithmetic average of the absolute values of the measured profile height deviations, *i.e.* the arithmetic roughness average, R_a , was equal to 7.82 nm and the maximum height of the profile above the mean line, R_p , was equal to 22.27 nm.

In the solution containing H_2SeO_3 , the presence of the distinct chain-like structures (not observed in the absence

of this additive) (Fig. 5b) somewhat resembles the surface morphology of a Cu-precovered Pt(poly) electrode [21]. These structures were found to be composed of numerous separate particles. In the zone surrounding these structures, a rather homogeneous distribution of elongated clusters and separate particles can be seen (Figs. 5d and 7) with a density of about $6 \cdot 10^9 \text{ cm}^{-2}$. Consequently, the values of N obtained from the AFM images are about two orders larger than those from analysis of the transients (Table). This is likely due to the formation of multiple nuclei within a single diffusion zone. Nevertheless,

the physical origin of this discrepancy should be studied in more detail.

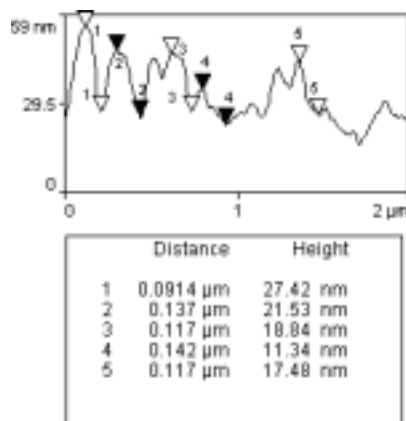


Fig. 6. Cross-sectional profile along a selected line (from Fig. 5c)

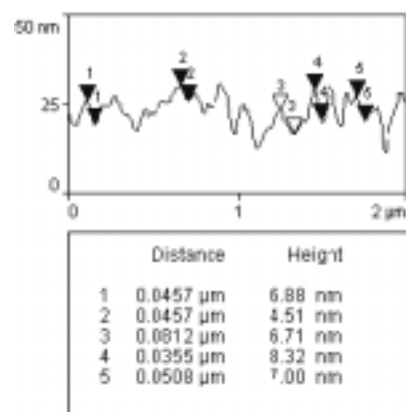


Fig. 7. Cross-sectional profile along a selected line (from Fig. 5d)

The growth of the clusters and particles was found to be favoured in the x - y directions rather than in the z -direction, especially in the case of the solution containing H_2SeO_3 , when the ratio x/z was increased by *ca.* 24 % (Figs. 6 and 7). The parameters R_a and R_p were of less magnitudes – 3.14 and 8.00 nm, respectively, indicating a rather strong smoothening effect of H_2SeO_3 .

The actual charge involved in Cu electrodeposition (Fig. 5c,d) was calculated by integration of the area in the corresponding transients, as mentioned above; these values were 15.5 mC in the absence of H_2SeO_3 and 12.3 mC in the presence of the additive. Both values of Q are markedly smaller than those expected from the AFM data if the nuclei were hemispherically shaped, 23 and 58.7 mC respectively. Such a discrepancy between the charges may indicate that the Cu growing centers are not hemispherical as, indeed, followed from the values of the parameter x/z .

The presence of some areas of the Pt substrate, which remained uncovered with Cu during electrodeposition, was also revealed at a more detailed inspection of the AFM images (Figs. 5–7).

CONCLUDING REMARKS

In this study, the initial stages of Cu electrodeposition onto Pt(poly) were investigated in acidic CuSO_4 solution without or with H_2SeO_3 when the molar concentration ratio $[\text{Cu(II)}]/[\text{Se(IV)}]$ was no less than $2 \cdot 10^2$. The combination of electrochemical experiments (cyclic voltammetry and potential step) and morphological observations (AFM) was performed to analyse the mechanism of nucleation and growth.

The analysis of the electrochemical results indicated that the Cu electrodeposition onto Pt(poly), precovered with underpotentially deposited Cu adlayer begins through the instantaneous 3D nucleation and diffusion-controlled growth mechanism proposed by Scharifker and Hills. The values of the diffusion coefficient (D) for Cu^{2+} ion, the number of nuclei (N) being of the order of 10^6 to 10^5 cm^{-2} , and average radius (r_{av}) of nuclei were calculated from chronoamperometric data. It was obtained that N decreased and r_{av} increased with increasing the bulk concentration of H_2SeO_3 . This is likely due to the so called CORC mechanism involving partial reduction of Cu^{2+} to an intermediate Cu^+ and consequently an increase in the concentration of Cu^+ at the surface of the electrode as proposed by Hill and Rogers.

The AFM observations showed that the Cu clusters were of comparable sizes and rather homogeneously distributed on the surface with the densities of about $9 \cdot 10^8 \text{ cm}^{-2}$ in the absence of H_2SeO_3 and

$6 \cdot 10^9 \text{ cm}^{-2}$ in the presence of 0.005 mM H_2SeO_3 . In the local regions of the surface, separate rather large agglomerates composed of clusters of different diameter were revealed in both cases, but in the presence of H_2SeO_3 such agglomerates attained a distinct chain-like configuration. The growth of clusters was found to be favoured in the x - y directions rather than in the z -direction, especially in the presence of H_2SeO_3 . The morphological characteristics were reported.

Received 09 July 2004

Accepted 16 August 2004

References

1. E. Budevski, G. Staikov and W. J. Lorenz, *Electrochemical Phase Formation and Growth*, VCH, Weinheim–New York–Basel–Cambridge–Tokyo (1996).
2. Yu. D. Gamburg, *Electrochemical Crystallization of Metals and Alloys*, Janus–K, Moscow (1997) (in Russian).
3. R. J. Nichols, W. Beckmann, H. Meyer, N. Batina and D. M. Kolb, *J. Electroanal. Chem.*, **330**, 381 (1992).
4. W. Plieth, *Electrochim. Acta*, **37**, 2115 (1992).
5. G. Fabricius, K. Kontturi and G. Sundholm, *Electrochim. Acta*, **39**, 2353 (1994).
6. V. V. Trofimenko and Yu. M. Loshkarev, *Elektrokimiya*, **30**, 150 (1994).
7. M. J. Llorca, E. Herrero, J. M. Feliu and A. Aldaz, *J. Electroanal. Chem.*, **373**, 217 (1994).
8. E. Herrero, A. Rodes, J. M. Pérez, J. M. Feliu and A. Aldaz, *J. Electroanal. Chem.*, **412**, 165 (1996).
9. R. N. Bhattacharya, A. M. Fernandez, M. A. Contreras, J. Keane, A. Tenant, K. Ramanathan, J. R. Tuttle, R. N. Noufi and A. M. Hermann, *J. Electrochem. Soc.*, **143**, 854 (1996).
10. D. Lippkow and H.-H. Strehblow, *Electrochim. Acta*, **43**, 2131 (1998).
11. P. Carbonnelle and L. Lamberts, *J. Electroanal. Chem.*, **340**, 53 (1992).
12. S. Massaccesi, S. Sanchez and J. Vedel, *J. Electrochem. Soc.*, **140**, 2540 (1993).
13. A. Marlot and J. Vedel, *J. Electrochem. Soc.*, **146**, 177 (1999).
14. M. Kemell, H. Saloniemi, M. Ritala and M. Leskelä, *Electrochim. Acta*, **45**, 3737 (2000).
15. M. R. Hill and G. T. Rogers, *J. Electroanal. Chem.*, **68**, 149 (1976).
16. T. I. Lezhava, *Acceleration at Metal Deposition*, Diss., A. N. Frumkin Inst. Electrochem., Moscow (1989).
17. A. Steponavičius, D. Šimkūnaitė and V. Jasulaitienė, *Chemija* (Vilnius), Nr. 2, 64 (1997).
18. G. Riveros, R. Henriquez, R. Córdova, R. Schrebler, E. A. Dalchiele and H. Gómez, *J. Electroanal. Chem.*, **504**, 160 (2001).
19. A. Steponavičius, D. Šimkūnaitė, S. Lichušina and V. Kapočius, *Chemija* (Vilnius), **12**, 147 (2001).

20. A. Steponavičius and D. Šimkūnaitė, *Bull. Electrochem.*, **18**, 367 (2002).
21. D. Šimkūnaitė, E. Ivaškevič, V. Jasulaitienė, A. Kaliničenko, I. Valsiūnas and A. Steponavičius, *Chemija (Vilnius)*, **15**, 12 (2004).
22. N. Furuya and S. Motoo, *J. Electroanal. Chem.*, **72**, 165 (1976).
23. D. Margheritis, R. C. Salvarezza, M. C. Giordano and A. J. Arvia, *J. Electroanal. Chem.*, **229**, 327 (1987).
24. D. Šimkūnaitė, E. Ivaškevič, V. Jasulaitienė and A. Steponavičius, *Bull. Electrochem.*, **19**, 437 (2003).
25. G. Jerkiewicz, Gh. Vatankhab, J. Lessard, M. P. Sorriaga and Y.-S. Park, *Electrochim. Acta.*, **49**, 1451 (2004).
26. D. Šimkūnaitė, A. Steponavičius, V. Jasulaitienė and E. Matulionis, *Trans. Inst. Met. Finish.*, **81**, 199 (2003).
27. S. Fletcher, C. S. Halliday, D. Gates, M. Westcott, T. Lwin and G. Nelson, *J. Electroanal. Chem.*, **159**, 267 (1983).
28. R. T. Carlin, W. Crawford and M. Bersch, *J. Electrochem. Soc.*, **139**, 2720 (1992).
29. B. Scharifker and G. Hills, *Electrochim. Acta*, **28**, 879 (1983).
30. B. R. Scharifker and J. Mostany, *J. Electroanal. Chem.*, **177**, 13 (1984).
31. D. Grujicic and B. Pesic, *Electrochim. Acta*, **47**, 2901 (2002).
32. A. Leone, W. Marino and B. R. Scharifker, *J. Electrochem. Soc.*, **139**, 438 (1992).
33. T. I. Quickenden and Q. Xu, *J. Electrochem. Soc.*, **143**, 1248 (1996).
34. J. Yu, L. Wang, L. Su, X. Ai and H. Yang, *J. Electrochem. Soc.*, **150**, C19 (2003).

**Dijana Šimkūnaitė, Emilija Ivaškevič,
Aleksandras Kaliničenko, Antanas Steponavičius**

**KAI KURIŲ PRIEDŲ ĮTAKA Cu SLUOKSNIŲ
FORMAVIMUISI POTENCIALŲ ZONOSE,
TEIGIAMESNĖSE IR NEIGIAMESNĖSE UŽ
PUSIAUSVYRINĘ SISTEMOS $\text{Cu}^{2+}/\text{Cu}^0$ POTENCIALO
REIKŠMĘ, RŪGŠČIUOSE CuSO_4 TIRPALUOSE
10. Cu NUSODINIMO ANT POLIKRISTALINĖS Pt
ESANT H_2SeO_3 PIRMŪJŲ STADIJŲ
VOLTAMPEROMETRINIS IR ATOMINĖS JĖGOS
MIKROSKOPINIS TYRIMAS**

S a n t r a u k a

Cu elektrolitinio nusodinimo pirmosios stadijos ant polikristalinės Pt substrato iš 0,5 M H_2SO_4 + 0,01 M CuSO_4 tirpalo, kurio H_2SeO_3 koncentracijos įvairios (visais atvejais koncentracijų santykis $[\text{Cu(II)}]/[\text{Se(IV)}]$ buvo ne mažesnis kaip $2 \cdot 10^2$), buvo tiriamos elektrocheminiais (ciklinė voltamperometrija ir potenciostatinis įjungimas) ir struktūriniais (atominės jėgos mikroskopija, AJM) metodais. Chronoamperometrinių rezultatų analizė parodė, kad Cu elektrolitinis nusodinimas ant Pt(poli) vyksta pagal momentinės 3D nukleacijos ir difuzijos kontroliuojamo užuomazgų augimo modelį, kurį pasiūlė Scharifker ir Hills. Iš šių duomenų taip pat apskaičiuotos Cu^{2+} jono difuzijos koeficiento D , susidariusių užuomazgų tankio N ir užuomazgų vidutinio spindulio r_{av} reikšmės. Parodyta, kad N mažėja, o r_{av} didėja, kai didėja tūrinė H_2SeO_3 koncentracija. AJM tyrimas parodė, kad nesant tirpale H_2SeO_3 ant Pt substrato paviršiaus, kuris dėl Pt išlaikymo elektrolite Cu ikištampinio nusodinimo potencialų zonoje (+0,35 V) pasidengė Cu adsluoksniu, susidaro atsitiktinai pasiskirstę maždaug vienodo dydžio Cu kristalitai. Atskirose paviršiaus vietose taip pat pastebėti gana dideli aglomeratai, sudaryti iš įvairaus skersmens kristalitų. Esant H_2SeO_3 , šie aglomeratai keičia savo formą, sudarydami į grandines panašias struktūras, o paviršiaus vietose apie pastarąsias struktūras ir toliau stebimas gana homogeninis pailgų kristalitų ir atskirų dalelių pasiskirstymas. Ir nesant, ir esant H_2SeO_3 Cu kristalitai labiau augo x - y kryptimis, negu z kryptimi, ypač tirpale, turinčiame H_2SeO_3 .